PNAS
www.pnas.org

Supplementary Information for

Bright Quantum Dots Emitting at ~ 1600 nm in the NIR-IIb Window for Deep Tissue Fluorescence Imaging

Mingxi Zhang, Jingying Yue, Ran Cui, Zhuoran Ma, Hao Wan, Feifei Wang, Shoujun Zhu, Ying Zhou, Yun Kuang, Yeteng Zhong, Dai-Wen Pang and Hongjie Dai

Hongjie Dai
Email: hdai1@stanford.edu

This PDF file includes:

Supplementary text
Figs. S1 to S13
Captions for Movies S1 to S3
References for SI reference citations

Other supplementary materials for this manuscript include the following:

Movies S1 to S3

www.pnas.org/cgi/doi/10.1073/pnas.1806153115

Supplementary Information Text

Materials and Methods

Materials. $PbCl_2$, CdO, and sulfur powder (sublimed) were purchased from Alfa. Oleylamine, oleic acid, 1-octadecene (ODE), tetrachloroethylene (TCE), poly(acrylic acid) (MW~1,800), N,N'-dicyclohexylcarbodiimide (DCC), N-(3-dimethylaminopropyl)-N′-ethylcarbodiimide hydrochloride (EDC), 2-(N-morpholino)ethanesulfonic acid (MES), hydrate were purchased from Sigma-Aldrich. Phosphate-buffered saline (PBS) was purchased from Hyclone. mPEG-amine (MW~5K) was purchased from Laysan Bio. 8-Arm PEG-amine (MW~40K) was purchased from Advanced BioChemicals. Other reagents were of analytical grade. Deionized ultra-filtered (DIUF) water was used in all needed experiments.

Synthesis of PbS QDs. The PbS QDs were synthesized with a modified procedure (1, 2). Sulfur precursor solution was prepared by mixing 0.08 g (5 mmol) of sulfur powder, and 7.5 mL of oleylamine in two-neck flask at 120 ^{o}C under argon for 30 min. Lead precursor solution 0.834 g (3 mmol) of $PbCl_2$ and 7.5 mL of oleylamine in a three-neck flask and degassing for 30 min under argon at 120 ^{o}C and then increased to 160 ^{o}C. 2.25 mL of the sulfur precursor solution (0.75 mmol of S) was injected into the Pb precursor solution (3 mmol of Pb) under stirring. The temperature was maintained at 160 ^{o}C throughout the reaction. After 30 min, the reaction was quenched by adding 10 mL of cold hexane and 20 mL ethanol. The products were collected by centrifugation and re-suspended in 10 mL hexane/20 mL oleic acid. The mixture was agitated for 10 min to remove excess sulfur from the products. The QDs were precipitated via centrifugation. This precipitation procedure with oleic acid was repeated 3 times until the supernatant was colorless. After centrifugation of the suspension and decantation of the supernatant, the QDs were re-suspended in ODE.

Synthesis of CSQDs. The PbS/CdS CSQDs were synthesized via cation-exchange procedure (3). CdO (1.2 g, 9.2 mmol), oleic acid (8 mL), and ODE (20 mL) were heated to 200 °C, purged with Ar, and then cooled down to 100 °C. 5 mL of previously prepared PbS QDs suspended in ODE was bubbled with Ar for 10 min, and then injected into the Cd precursor. The reaction flask was quenched with 5 mL cold hexane after the growth reaction was conducted at 100 °C for 30 min. PbS/CdS CSQDs were precipitated with ethanol and then re-dispersed in hexane.

Modification of CSQDs with oleyamine-branched polyacrylic acid (OPA). OPA was synthesized with a modified procedure (4, 5). Typically, 0.9 g of poly(acrylic acid) powder (average MW~1800) and 1.56 g DCC were transferred into a round-bottom flask. 10 mL of DMF was added to dissolve the mixture. About 1.2 mL of oleylamine were added dropwise into the reaction flask. The molar ratio of oleylamine to PAA is 30%. The solution was stirred overnight. The solution was stirred for 16 h. 50 mL of 0.5 M HCl were added to the reaction solution. The precipitate was separated by centrifugation and re-dissolved in 3 mL methanol solution. And then 20 mL 1 M HCl was added to the solution. The precipitate was separated by centrifugation. This procedure was repeated at least 5 times. The precipitate was dissolved in 5 mL chloroform and washed by 10 mL 1 M HCl. The organic phase was collected and dried over by anhydrous

Na_2SO_4. The chloroform was removed under vacuum, and the white solid was collected. The average Mw of OPA was ~ 3000 determined by gel permeation chromatography.

For surface modification (6), as-synthesized CSQDs (5.0 mg) were dissolved in 2.0 mL chloroform containing 15 mg of OPA. The mixture was stirred at room temperature for 30 min and the solvent was removed under vacuum by a rotary evaporator. The residue was then dissolved in 2 mL of 50 mM sodium carbonate solution under the sonication. The CSQDs were precipitated with ultracentrifuge at 50,000 rpm for 1 h, and washed three times with deionized water. The purified product was dissolved in pH 8.5 MES buffer (0.01 M) and stored at 4 °C.

PEGylation of CSQDs. OPA-modified CSQDs (5 mg) were dissolved in 20 mL pH 8.5 MES buffer (0.01 M). 15 mg of mPEG-amine (MW ~ 5K) and 5 mg of 8-Arm PEG-amine (MW ~ 40 K) with a molar ratio of 24: 1 were dissolved 1 mL MES, and gradually added to QDs solution with stirring. 10 mg of EDC was dissolved in 500 uL MES, and gradually added to QDs solution with stirring. The mixture was stirred at room temperature overnight. The PEGylated QDs was purified by 100 kDa filter, and washed five times with 1x PBS to remove excess reactants. The purified product was dissolved in 1x PBS and stored at 4 °C.

Characterizations. Transmission electron microscopy (TEM) images were obtained on a JEM-2100F electron microscope (JEOL) with an acceleration voltage of 200 kV. The TEM samples were prepared by drying a hexane dispersion of the QDs on copper grids coating with amorphous carbon film. High-angle annular dark-field scanning TEM (HAADF-STEM) and energy dispersive spectroscopy (EDS) mapping images were obtained on a FEI Titan Cubed Themis G2 300 with a probe corrector and operated at 60 kV. The X-ray powder diffraction (XRD) patterns were obtained on a Bruker D8 Advanced X-Ray diffractometer (Bruker AXS) using Cu K-alpha radiation of wavelength 1.5406 **Å**, and the scan rate was 0.5 degree/min. Energy-dispersive X-ray (EDX) data was obtained by using JEM 2010F microscope equipped with EDX spectrometry (EDAX Inc.). UV-Vis-NIR absorbance spectra were measured on a Cary 6000i UV-Vis-NIR spectrophotometer. Dynamic light scattering (DLS) data were recorded on a Malvern Nano-ZS ZEN3600 zetasizer. Inductively coupled plasma atomic absorption spectrometry (ICP-AAS) data were obtained on a Hitachi Z-2000 atomic absorption spectrophotometer. The NIR fluorescence spectra were measured using the same home-built NIR fluorescence spectrometer. The excitation was provided by an 808-nm fiber-coupled diode laser (RPMC Lasers) and filtered with selected short-pass filters. The excitation light was directed to pass through a 1-mm path cuvette containing sample solution. The emission light was filtered using a 900-nm long-pass filter (Thorlabs) to reject the excitation light and then directed into a spectrometer (Acton SP2300i, USA) equipped with a liquid-nitrogen-cooled InGaAs linear array detector (Princeton Instruments, OMA-V, USA). All the raw emission spectra in this study were corrected for the detector sensitivity and extinction features of the filters.

Animal handling. All animal experiments were performed under the approval of Stanford University's Administrative Panel on Laboratory Animal Care. Eight-week-old female C57BL/6 mice were obtained from Charles River for imaging studies and housed at the Research Animal Facility of Stanford under our approved animal protocols. Before imaging, all mice were anaesthetized in a rodent anesthesia machine with 2 l min^{-1} O_2 gas mixed with 3% isoflurane. During the time course of imaging the mouse was kept anaesthetized by a nose cone delivering 2 l min^{-1} O_2 gas mixed with 3% isoflurane.

***In vivo* wide-field fluorescence imaging in the NIR-IIb window.** NIR-II fluorescence images were recorded using a 2D liquid-nitrogen cooled InGaAs camera (Princeton Instruments 2D OMA-V, USA). Mice were placed on a stage with a venous catheter for injection. An 808 nm fiber-coupled diode laser (RPMC Lasers, USA) with a power density of 60 mW/cm^2 was used as

the excitation source and an excitation filter set (850 and 1000 nm short-pass filters) was used to filter the excitation light. A lens set (1X, 2.5X, 10X) was used to obtain tunable magnifications. The NIR-IIb imaging was done after an intravenous injection of CSQDs dispersed in PBS buffer (200 μL, 2 mg/mL). The emitted fluorescence from CSQDs were directed onto the InGaAs camera through an emission filter set (1100 nm and 1500 nm long-pass filters) to select the NIR-IIb window respectively. The video-rate imaging of hindlimb was performed using Ninox 640 cooled InGaAs camera (Raptor) with an exposure time of 5 ms (laser power density: ~70 mW/cm^2). The video-rate imaging of brain and heart/lung was performed using 2D liquid-nitrogen cooled InGaAs camera (Princeton Instruments) with an exposure time of 2 ms (laser power density: ~60 mW/cm^2). All images were processed with MATLAB.

***In vivo* confocal fluorescence imaging in the NIR-IIb window.** For obtaining *in vivo* confocal hindlimb and tumor imaging data, we used a home-built stage scanning confocal setup. The 100X objective (Olympus, NA 0.8) focused 785 nm excitation laser with a power of 40 mW tightly on an anesthetized mouse injected with QDs dispersed in PBS buffer (200 μL, 2 mg/mL), and fluorescence from QDs passed a 1050 nm long-pass dichroic mirror and 1500 nm long-pass filter before being collected by an NIR PMT (Hamamatsu, 12397-75). A 150 μm pinhole was used to exclude out of focus fluorescence. For 2000 μm x 2000 μm, 800 μm x 800 μm, and 300 μm x 300 μm images, the pixel size was 10 μm, 5 μm and 2 μm respectively, and the frame rate was 7 min/frame, 5 min/frame, and 5 min/frame respectively. The mouse recovered well after scanning for a few hours.

***In vivo* pharmacokinetics and biodistribution of QDs.** C57 mice were used for pharmacokinetics and biodistribution studies with 3 mice for each experiment. All mice were intravenously injected with PEG-QDs in PBS buffer (200 μL, 2 mg/mL). At time points of 2, 4, 6, 8, 10, 24, 48 and 72 h p.i., 50 μL blood were collected using a capillary tube stuck into the corner of one eye, and then diluted with EDTA-Na_2 solution (40 mg/mL). The percentage of the QDs in blood was estimated by calculating the Pb atom concentration in blood using inductively coupled plasma atomic absorption spectrometry (ICP-AAS). Biodistribution was performed after 2 h, 24 h and 72 h p.i.. Main organs including heart, liver, spleen, lung, kidney, stomach and gut were collected. For excretion experiment, the feces were collected for 28 days. The organs and feces were weighed and then dissolved in 5 mL digest solution (HNO_3 : H_2O_2 = 4:1). The samples were heated to 220 °C for 2 h. The reaction stopped when the solution became clear and then cooled down to room temperature. Each of the resulting solutions was diluted by deionized water to 10 mL, and subsequently analyzed by ICP-AAS to determine the concentration of Pb atom in each sample. The calculation formula is: % ID/g= (The amount of Pb atom in organs or feces) / (The amount of Pb atom in injected solution × the mass of organs or feces) × 100%.

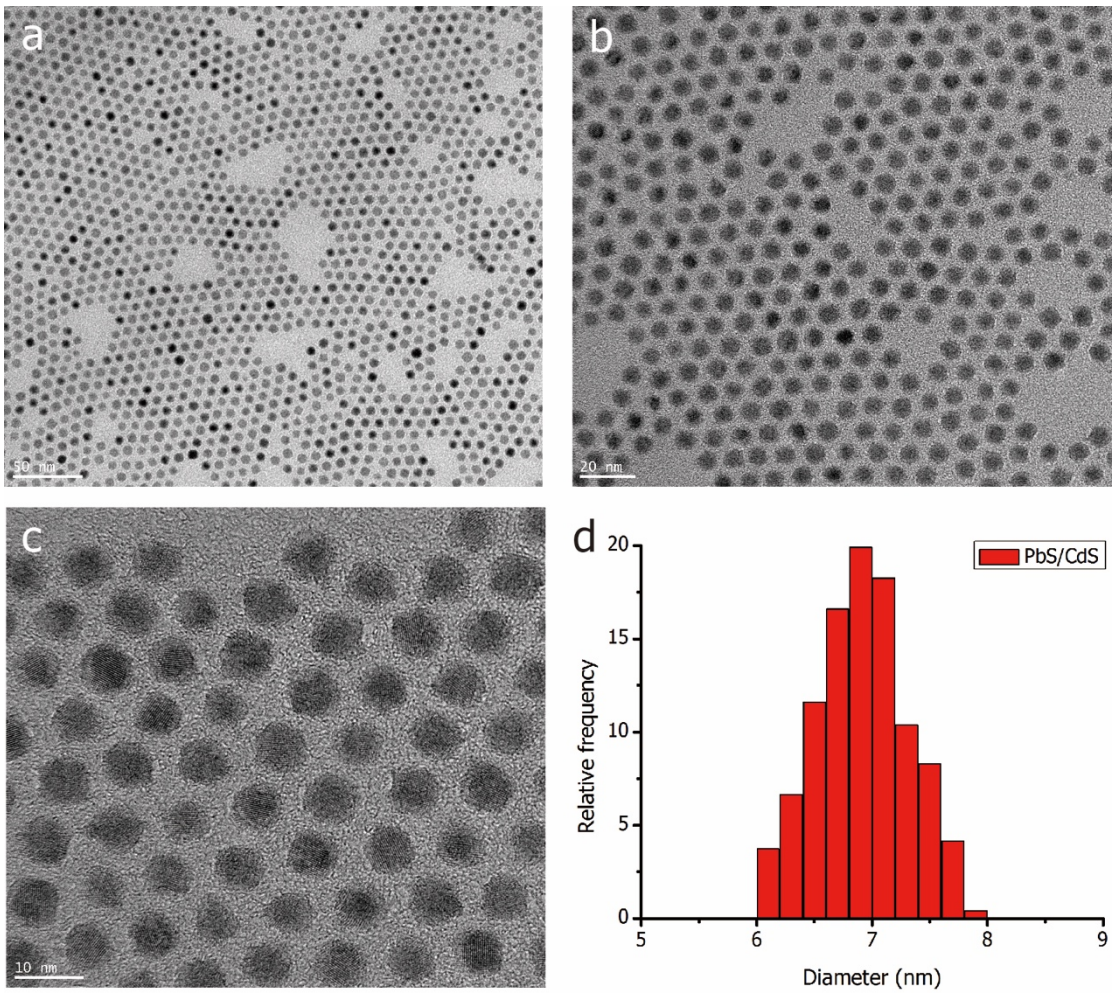

Fig. S1. (a-c) TEM images of as-prepared core/shell PbS/CdS CSQDs. The scale bars are 50 nm (a), 20 nm (b), and 10 nm (c), respectively. (d) Size-distribution histogram of CSQDs (n=300).

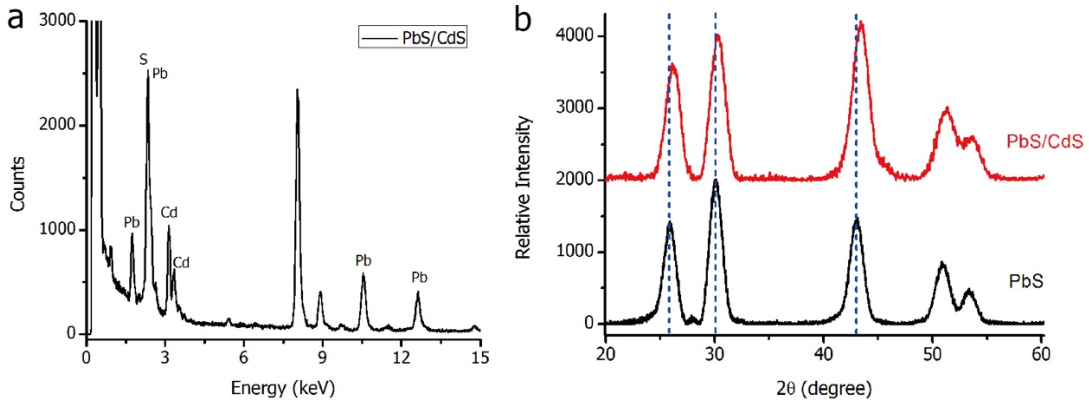

Fig. S2. (a) Energy-dispersive X-ray (EDX) of core/shell PbS/CdS CSQDs. (b) X-ray powder diffraction (XRD) spectra of the precursor PbS QDs (black curve) and the core/shell PbS/CdS CSQDs (red curve).

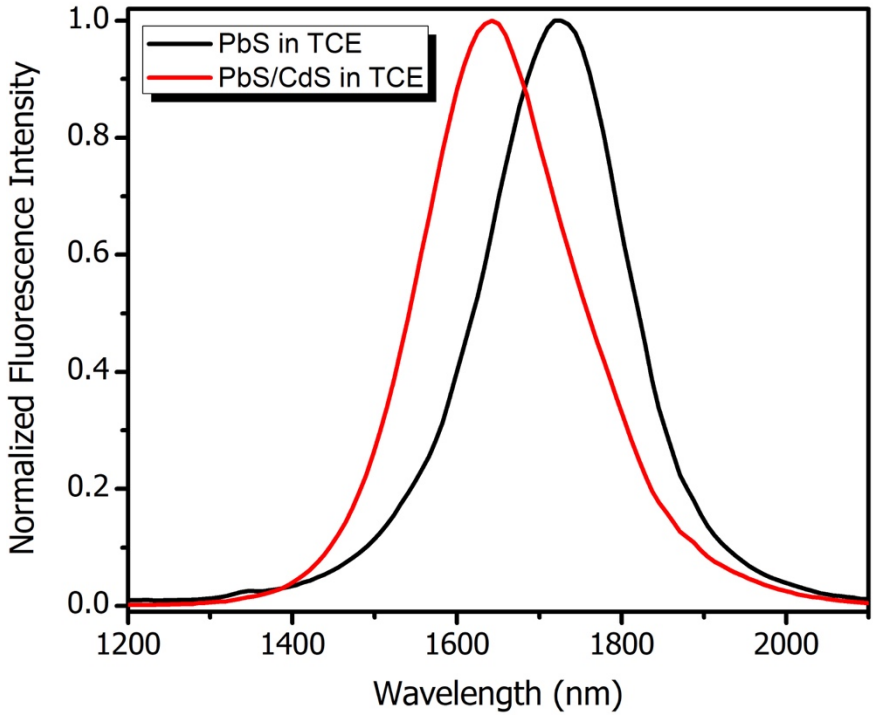

Fig. S3. Fluorescence emission spectra of the precursor PbS QDs (black curve) and the core/shell PbS/CdS CSQDs (red curve) in tetrachloroethylene (TCE).

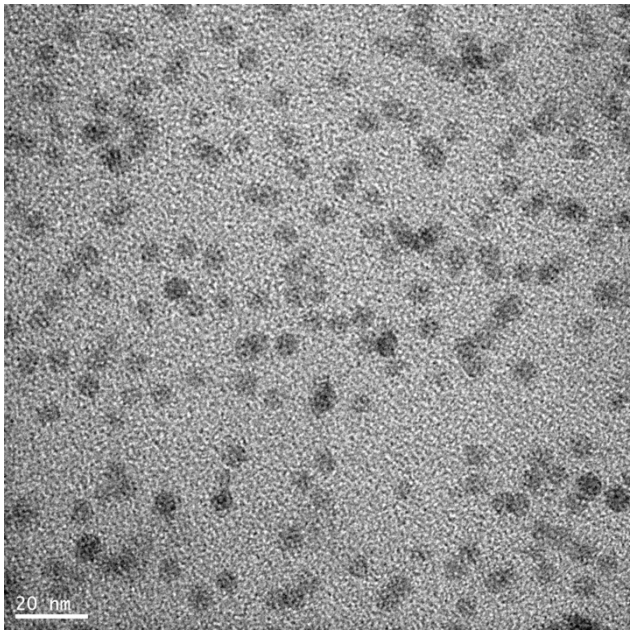

Fig. S4. TEM images of PEG-CSQDs. The scale bars are 20 nm.

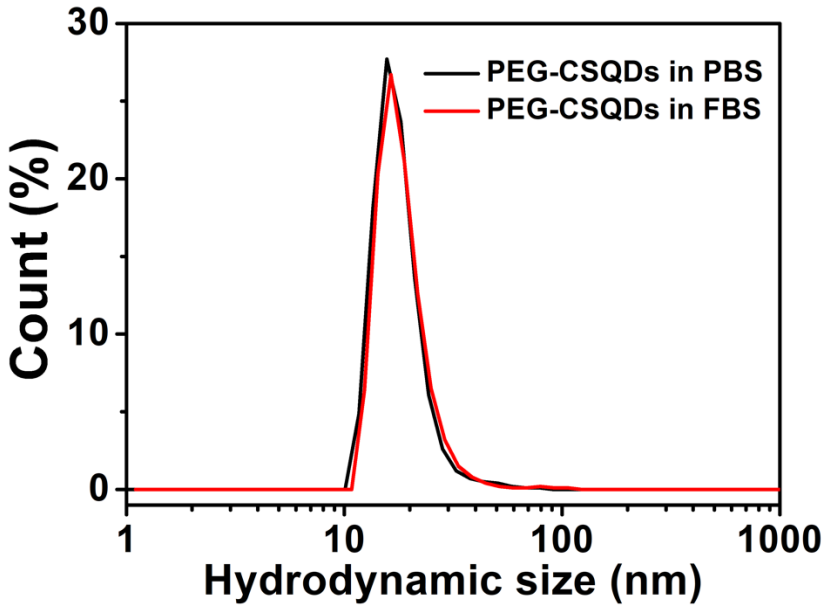

Fig. S5. Dynamic light scattering spectra of PEG-CSQDs in PBS and FBS.

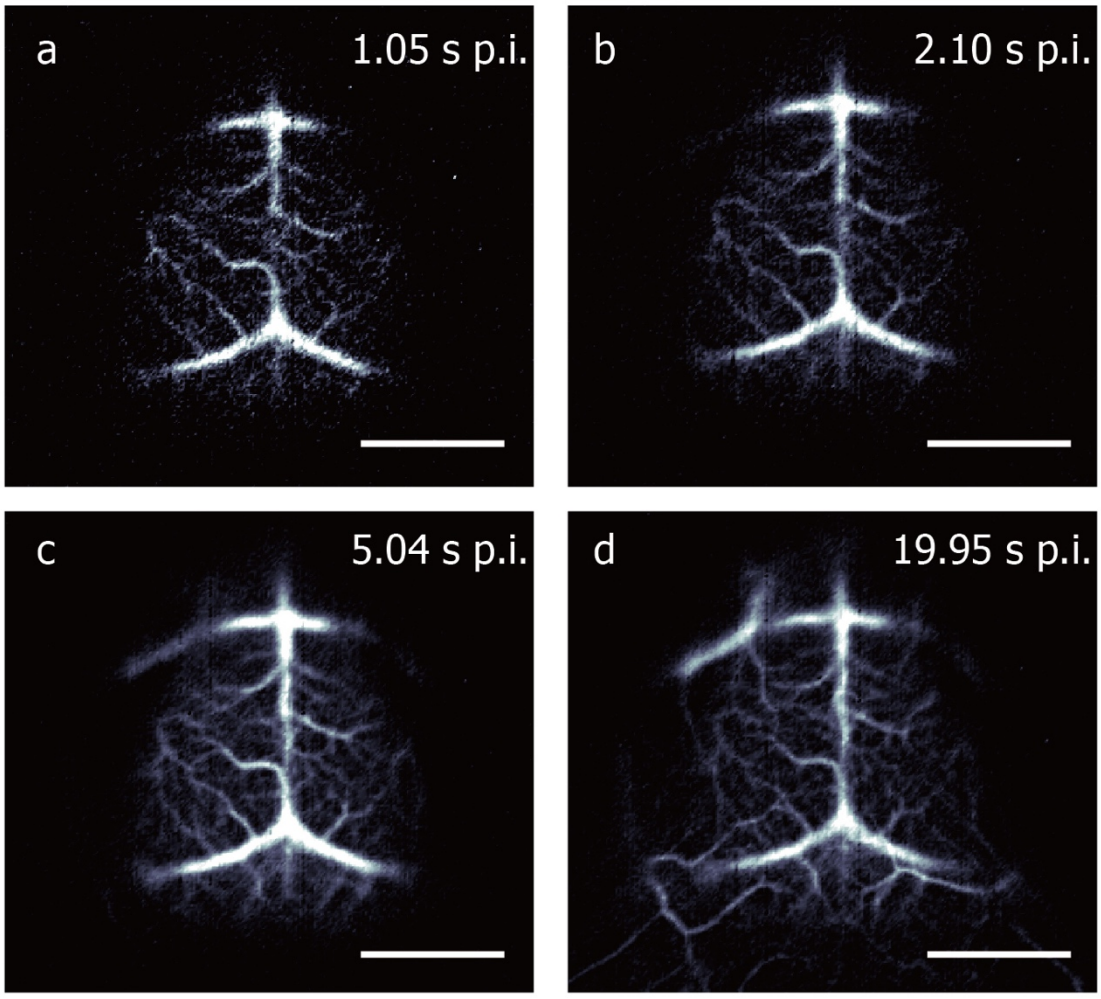

Fig. S6. Selected time points from video-rate fluorescence imaging of mouse cerebral vessels at ~ 1600 nm after an intravenous injection of PEG-CSQDs (808 nm laser excitation, 2.5X objective, 1500 nm long-pass filter, 2 ms exposure time using an OMA-V liquid-nitrogen-cooled InGaAs camera, laser power density ~ 60mW/cm^2). The scale bar is 5 mm. See Movie S2.

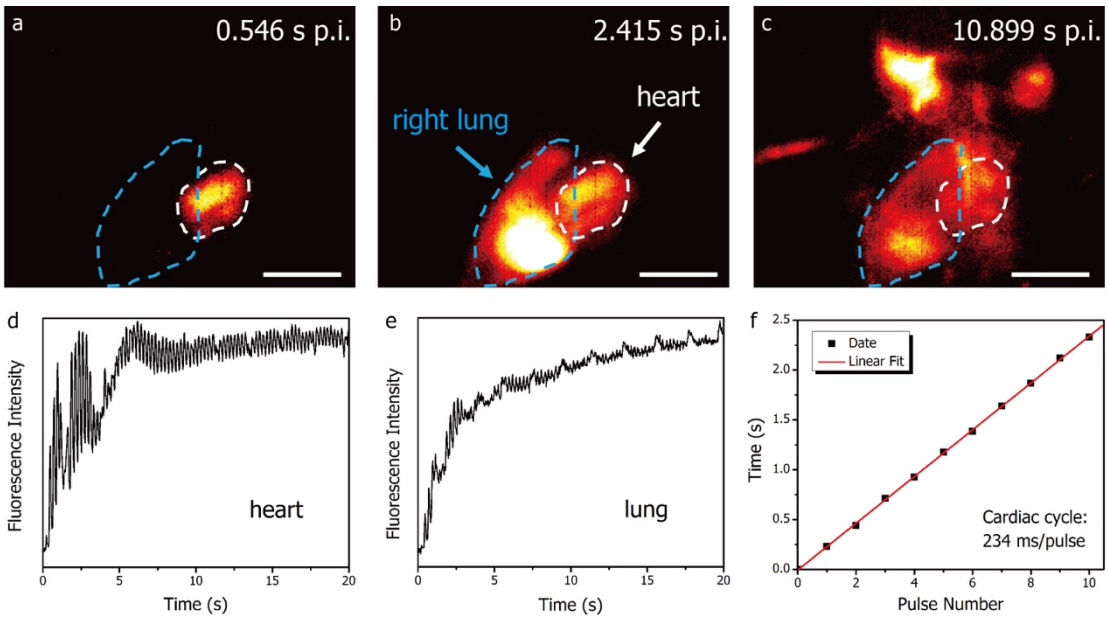

Fig. S7. Real-time visualizing of mouse heart/lung hemodynamics. (a-c) Selected time points from video-rate fluorescence imaging of mouse heart/lung at ~ 1600 nm after an intravenous injection of PEG-CSQDs (808 nm laser, 2.5X objective, 1500 nm long-pass filter, 2 ms exposure time an OMA-V liquid-nitrogen-cooled InGaAs camera, laser power density ~ 60mW/cm^2, laser power density~60 mW/cm^2). The scale bar is 5 mm. Fluorescence intensity changes in heart (d) and lung (e) regions over time during the real-time video-rate NIR-IIb imaging using PEG-CSQDs. (f) Linear fit of time of the periodic variations over heart pulses revealing a cardiac cycle of 243 ms per cardiac cycle. See Movie S3.

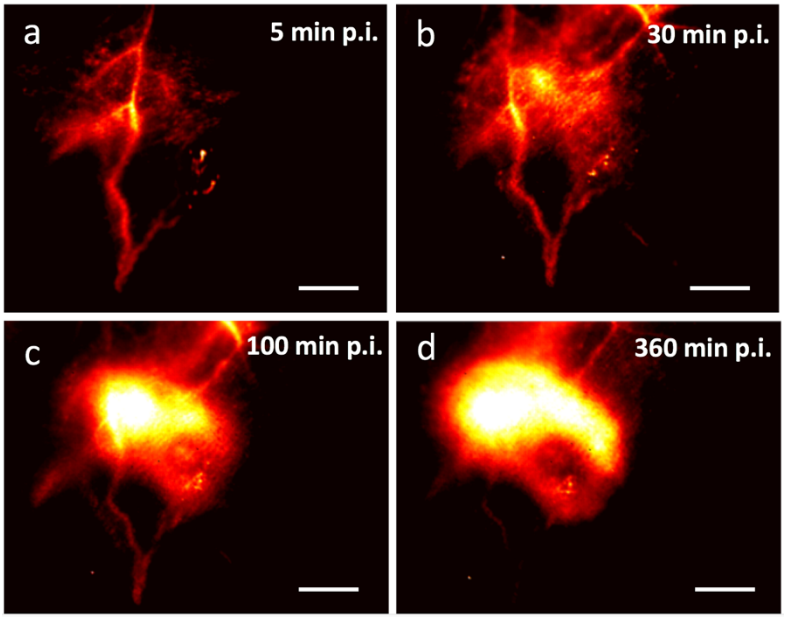

Fig. S8. High magnification (10X objective) wide-field fluorescence imaging of a mouse with a xenograft MC38 tumor after tail-vein intravenous injection of PEG-CSQDs at different p.i. time points. The scale bar is 1 mm. Imaging experiment parameters: 808 nm laser, 1500 nm long-pass filter, laser power density ~ 60 mW/cm^2.

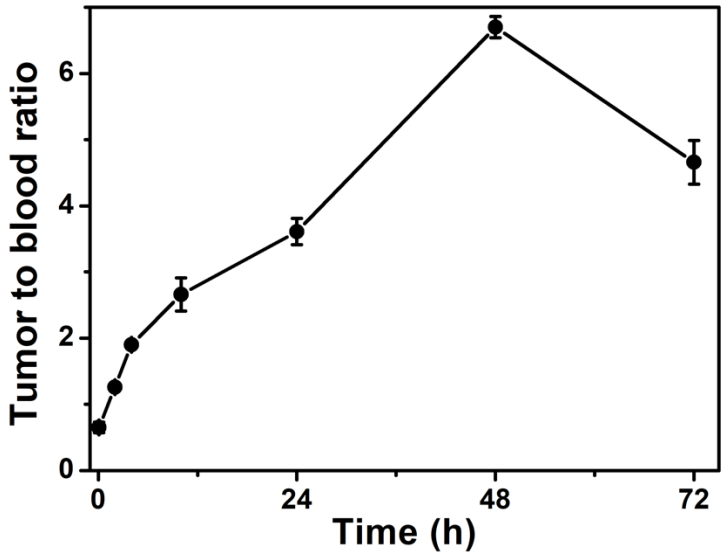

Fig. S9. Time-course curve of tumor-to-blood ratios of a mouse with xenograft MC38 tumor after intravenous injection of PEG-CSQDs over 96 h p.i.

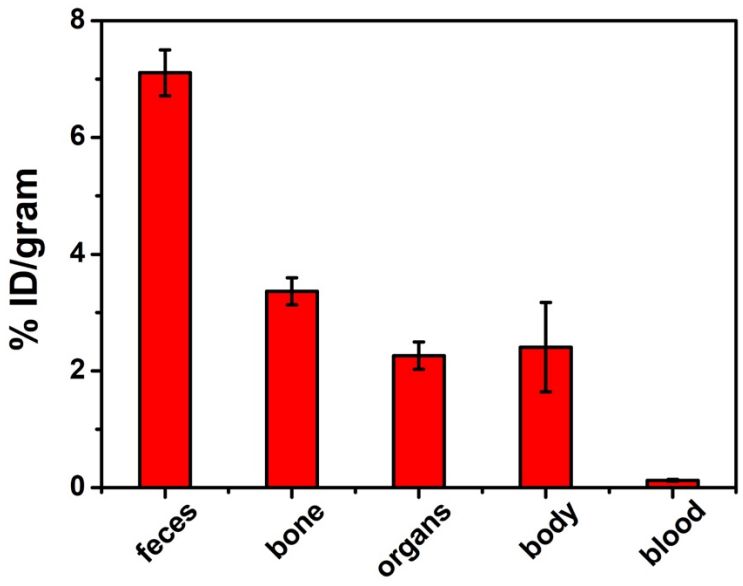

Fig. S10. Biodistribution of CSQDs in different parts of treated mice after 7-day p.i.. All of feces during 7 days were collected. Organs: heart, liver, spleen, lungs, kidneys, stomach, gut. Body: other parts of mouse, including skin, muscle, brain, *et al.*

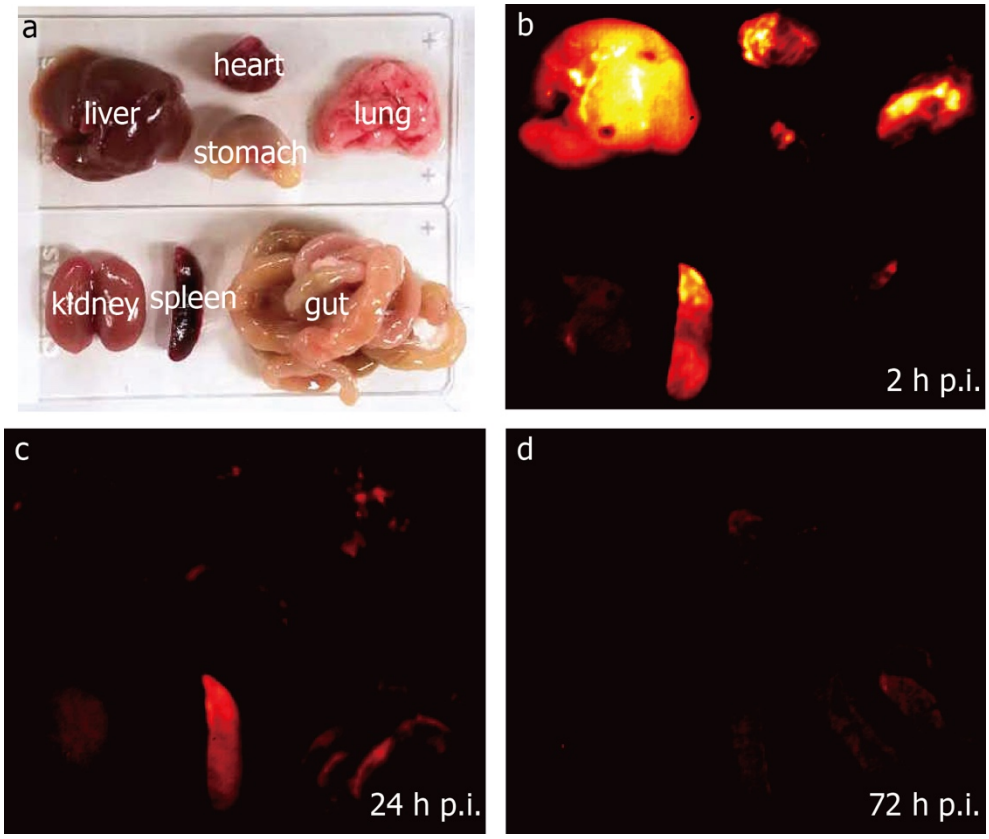

Fig. S11. Wide-field bright image (a) and fluorescence images of main organs from PEG-CSQDs treated mice taken 2 h (b), 24 h (c), and 72 h (d) p.i..

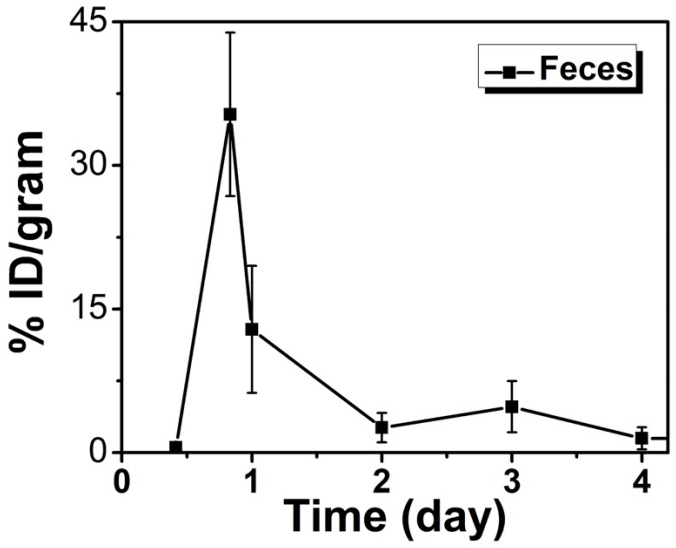

Fig. S12. Time-course of CSQDs concentration in the feces of mouse treated with PEG-CSQDs over 96 h p.i..

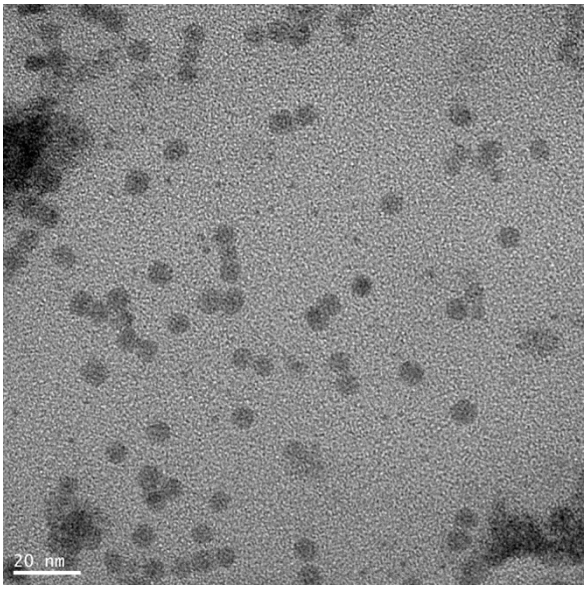

Fig. S13. TEM image of CSQDs separated from feces. The scale bar is 20 nm.

Movie S1. Video-rate fluorescence imaging at ~ 1600 nm showing the blood flow returning to the femoral vein after filling the femoral artery. The observed NIR-II fluorescence signals come from PEG-CSQDs. t = 0 is defined as the time point when NIR-IIb signal started to show up in the femoral vein. The frame rate of imaging is 60 fps (808 nm laser excitation, 2.5X objective, 1500 nm long-pass filter, 5 ms exposure time using a Ninox 640 InGaAs camera, laser power density ~ 70 mW/cm^2).

Movie S2. Video-rate fluorescence imaging of mouse cerebral vessels at ~ 1600 nm after an intravenous injection of PEG-CSQDs. The observed NIR-II fluorescence signals come from PEG-CSQDs (808 nm laser excitation, 2.5X objective, 1500 nm long-pass filter, 2 ms exposure time using an OMA-V liquid-nitrogen-cooled InGaAs camera, laser power density ~ 60mW/cm^2).

Movie S3. Video-rate fluorescence imaging of mouse heart/lung at ~ 1600 nm after an intravenous injection of PEG-CSQDs. The observed NIR-II fluorescence signals come from the PEG-CSQDs (808 nm laser excitation, 2.5X objective, 1500 nm long-pass filter, 2 ms exposure time using an OMA-V liquid-nitrogen-cooled InGaAs camera, laser power density ~ 60mW/cm^2).

References

1. Cademartiri L*, et al.* (2006) Multigram Scale, Solventless, and Diffusion-Controlled Route to Highly Monodisperse PbS Nanocrystals. *J. Phys. Chem. B* 110:671-673.
2. Moreels I*, et al.* (2011) Size-Tunable, Bright, and Stable PbS Quantum Dots: A Surface Chemistry Study. *ACS Nano* 5:2004-2012.
3. Neo MS, Venkatram N, Li GS, Chin WS, & Ji W (2010) Synthesis of PbS/CdS Core-Shell QDs and their Nonlinear Optical Properties. *J. Phys. Chem. C* 114:18037-18044.
4. Zhou M*, et al.* (2007) Peptide-Labeled Quantum Dots for Imaging GPCRs in Whole Cells and as Single Molecules. *Bioconjugate Chem.* 18(2):323-332.
5. Zhang M-X, Huang B-H, Sun X-Y, & Pang D-W (2010) Clickable Gold Nanoparticles as the Building Block of Nanobioprobes. *Langmuir* 26(12):10171-10176.
6. Pellegrino T*, et al.* (2004) Hydrophobic Nanocrystals Coated with an Amphiphilic Polymer Shell: A General Route to Water Soluble Nanocrystals. *Nano Lett.* 4:703-707.